

# Phase sensitive quantum interference on forbidden transition in ladder scheme

Gennady A. Koganov\*, Reuben Shuker

*Physics Department, Ben-Gurion University of the Negev,  
P.O.B. 653, Beer Sheva, 84105, Israel*

---

## Abstract

A three level ladder system is analyzed and the coherence of initially electric-dipole forbidden transition is calculated. Due to the presence of two laser fields the initially dipole forbidden transition becomes dynamically permitted due to ac Stark effect. It is shown that such transitions exhibit quantum-interference-related phenomena, such as electromagnetically induced transparency, gain without inversion and enhanced refractive index. Gain and dispersion characteristics of such transitions strongly depend upon the relative phase between the driving and the probe fields. Unlike allowed transitions, gain/absorption behavior of ac-Stark allowed transitions exhibit antisymmetric feature on the Rabi sidebands. It is found that absorption/gain spectra possess extremely narrow sub-natural resonances on these ac Stark allowed forbidden transitions. An interesting finding is simultaneous existence of gain and negative dispersion at Autler-Townes transition which may lead to both reduction of the group velocity and amplification of light.

**Keywords:** Quantum interference, Gain without inversion, Enhanced refraction index

---

## 1. Introduction

Phase sensitive detection is of major importance in physical quantity measurements. A number of works on phase sensitive phenomena, both theoretical and experimental have been published recently (see, e.g. Refs. [1–4] and references therein). In this paper we investigate quantum control and interference in a three level ladder system. This approach can be extended to other schemes and generalized to more levels. High dependence and sensitivity on the relative phase of the pump and probe em modes of the relevant lasers is found and presented here. This sensitivity is particularly accentuated in the third transition, whose frequency is essentially the sum of the frequencies of the sequential transitions in the ladder, even when this transition is one photon emission forbidden in the bare state [5], i.e., without the presence of the pump and probe fields. Similarly to semiconductor structures [2, 6–8], where all three transitions in the ladder three level scheme are allowed due to dc Stark mixing, in atomic ladder system the initially

forbidden transition becomes dynamically allowed due to ac Stark mixing. Recently experimental evidence of such an effect was reported [9]. A most interesting finding is that the effect of such phase control renders amplification, absorption and dispersion at will on an initially unallowed transition. Moreover, subnatural linewidth resonances are found, which can be detuned from both Autler-Townes [10] and bare resonances. Phase control provides a key for detection, amplification, enhanced dispersion as well as anomalous negative index of refraction, dark states and other quantum characteristics. Our findings are not limited to the ladder scheme but rather also applicable, with the proper modifications, to the  $\Lambda$  and V schemes which are shown in Fig.1.

In order to provide physical intuition and understanding, electric dipole forbidden transition, becomes allowed by ac Stark mixing with other allowed transitions as a result of the strong electric field of the impinging electromagnetic radiation, as detailed below. Gain without inversion at the third transition in the ladder scheme is of particular interest in the X-Ray regime, where coherent sources are scarce.

Quantum-interference-related phenomena, such as electromagnetically induced transparency (EIT), lasing

---

\*Corresponding author: Gennady Koganov  
Email addresses: quant@bgu.ac.il (Gennady A. Koganov), shuker@bgu.ac.il (Reuben Shuker)

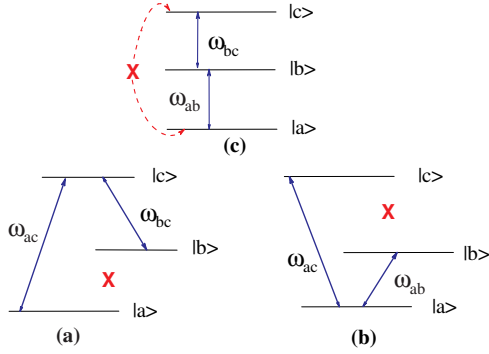


Figure 1: Schematic  $\Lambda$  (a),  $V$  (b) and ladder (c) three level configurations. Transitions  $|a\rangle \rightarrow |b\rangle$ ,  $|b\rangle \rightarrow |c\rangle$  and  $|a\rangle \rightarrow |c\rangle$  are initially dipole-forbidden (marked with red cross).

without inversion (ScullyBook) etc., are based on the interference between two independent quantum channels [11–17]. Traditional treatment of such phenomena typically involves a three level scheme and two coherent fields, a strong driving field and a weak probe one, applied to the two dipole-allowed transitions, followed by measurement of the absorption and the dispersion of the probe transition.

We show in the following that dipole-forbidden transitions can also exhibit amplification, enhanced dispersion and other coherent phenomena. The electric field component of the driving laser field breaks the space spherical symmetry and renders the parity not well defined, as in  $dc$  Stark effect. In other words, the presence of a strong driving field exerts  $ac$  Stark effect and thus breaks the spherical symmetry of the system and creates an infinite ladder of dressed states [18, 19], so that transitions between the dressed states are not necessarily constrained by the selection rules for a free atomic system. An interesting signature of the forbidden transitions is the antisymmetric character of the gain and dispersion properties of such transitions are phase sensitive as they strongly depend upon the relative phase between the driving and probe fields. Our results open a perspective for new type of phase sensitive spectroscopy in a wide spectral range, from microwave to X-ray frequencies.

## 2. Hamiltonian, master equation and dressed states

There are three possible closed-loop three-level configurations,  $\Lambda$ ,  $V$  and the ladder schemes. These are shown in Fig. 1. All of the three schemes possess a

common property that due to selection rules, one of the three transitions is dipole-forbidden by parity which is well defined in the absence of the laser fields. However, the parity becomes ill defined due to the presence of the  $ac$  electric fields of the two impinging lasers. These fields break the space symmetry and mix states of different parity. Hence the originally forbidden transition becomes undefined. In this sense it becomes *dynamically* allowed. We call such dynamically allowed transitions *ac-Stark allowed* (ACSA) transitions. In a sense this is a different variant than the usual EIT or LWI schemes as here the transition is forbidden to begin with and there is no issue of population inversion. Such a possibility would be particularly important in the X-Ray regime for gain in a ladder scheme [20]. Other examples are forbidden transitions in Alkali atoms.

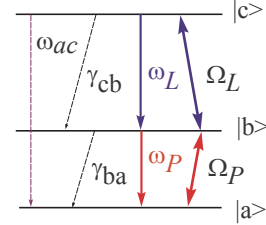


Figure 2: Schematic ladder three level configuration. Transitions  $|a\rangle \rightarrow |b\rangle$  and  $|b\rangle \rightarrow |c\rangle$  are dipole allowed, while the transition  $|a\rangle \rightarrow |c\rangle$  is initially dipole-forbidden.  $\omega_P/\omega_L$  and  $\Omega_P/\Omega_L$  are optical and Rabi frequencies of the probe/drive fields, respectively,  $\omega_{ac}$  is the energy difference between the levels  $|c\rangle$  and  $|a\rangle$ , not the transition frequency in the bare scheme.  $\gamma_{ba}$  and  $\gamma_{cb}$  are the rates of spontaneous emission on the two relevant allowed transitions

Without loss of generality among the three above mentioned configurations, we consider the Ladder-configuration (see Fig. 2). A strong driving field with frequency  $\omega_L$  is applied to atomic transition  $|b\rangle \rightarrow |c\rangle$ , and a probe field with frequency  $\omega_P$  is applied to atomic transition  $|a\rangle \rightarrow |b\rangle$ . The time dependent interaction Hamiltonian in the interaction picture is given by

$$H_{int} = \hbar\Omega_P e^{i(\Delta_P t + \varphi_P)} \sigma_{ab} + \hbar\Omega_L e^{i(\Delta_L t + \varphi_L)} \sigma_{bc} + H.c. \quad (1)$$

where  $\sigma_{ab} = |b\rangle\langle a|$ ,  $\sigma_{bc} = |c\rangle\langle b|$ , and  $\sigma_{ac} = |c\rangle\langle a|$  are the atomic rising operators,  $\Omega_L$  and  $\Omega_P$  are Rabi frequencies of the driving and the probe fields, respectively,  $\Delta_L$  and  $\Delta_P$  are detunings of the fields from corresponding atomic transitions. We emphasize the introduction of the phases  $\varphi_L$  and  $\varphi_P$  of the driving and the probe fields introduced explicitly in the Hamiltonian. The master

equation is given by

$$\frac{\partial \rho}{\partial t} = -\frac{i}{\hbar} [H_{int}, \rho] + \frac{1}{2} [\gamma_{ba}(2\sigma_{ba}\rho\sigma_{ab} - \sigma_{ab}\sigma_{ba}\rho) + \gamma_{cb}(2\sigma_{cb}\rho\sigma_{bc} - \sigma_{bc}\sigma_{cb}\rho)] \quad (2)$$

To analyze the steady state we eliminate the time dependence using the rotating wave approximation, then the system Hamiltonian is given by

$$H = \begin{pmatrix} 0 & \Omega_L e^{i\varphi_L} & 0 \\ \Omega_L e^{-i\varphi_L} & \Delta_L & \Omega_P e^{i\varphi_P} \\ 0 & \Omega_P e^{-i\varphi_P} & \Delta_L + \Delta_P \end{pmatrix} \quad (3)$$

where  $\Omega_P$  and  $\Omega_L$  are Rabi frequencies of the probe and the driving fields, respectively, and  $\Delta_P$  and  $\Delta_L$  are corresponding detunings. Abbreviated manifold of dressed states created by the strong driving field  $\Omega_L$  is shown in Fig. 3. The corresponding semiclassical dressed states in the case of two-photon resonance, i.e.  $\Delta_P + \Delta_L = 0$  are given by

$$|\pm\rangle = \frac{1}{\sqrt{2}} \left( \frac{\Omega_P}{\sqrt{\Omega_L^2 + \Omega_P^2}} |a\rangle \pm e^{-i\varphi_P} |b\rangle + \frac{e^{-i(\varphi_P + \varphi_L)} \Omega_L}{\sqrt{\Omega_L^2 + \Omega_P^2}} |c\rangle \right) \quad (4)$$

These dressed states are superposition of states of different parity and hence are not constrained by the selection rules for atomic states  $|a\rangle$ ,  $|b\rangle$ , and  $|c\rangle$ . As will be seen in the following, maximal gain is achieved when the probe and the drive lasers are in "dressed" two-photon resonance with transitions between the dressed states marked with red and orange arrows, i.e. at  $\Delta_P + \Delta_L = \pm R$ , where  $R = \sqrt{\Omega_P^2 + \Omega_L^2}$  is the generalized Rabi frequency.

### 3. Steady state coherences

We have solved analytically master equation (2) for the atomic density matrix  $\rho$  with the Hamiltonian (3) in steady state and calculated the coherences  $\rho_{ab}$  and  $\rho_{ac}$  on the probe and the ACSA transitions, whose imaginary and real parts are related to absorption/gain and dispersion, respectively. The main features can be qualitatively understood from the approximate expressions for the coherences  $\rho_{ab}$  and  $\rho_{ac}$  on probe and ACSA transitions at small probe field  $\Omega_P \ll \Omega_L$ , although all graphical results presented in the following have been obtained

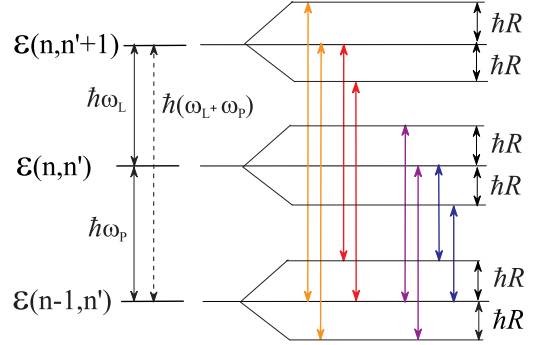


Figure 3: Dressed states picture at bare two-photon resonance  $\Delta_P + \Delta_L = 0$ . On the left: manifold of bare states labeled by the atomic level index  $a$ ,  $b$ , or  $c$ , the probe field photon number  $n$ , and the driving field photon number  $n'$ . On the right: dressed states of coupled atom+field system. Strong phase sensitive gain without inversion is obtained on the ACSA transition  $|a\rangle \rightarrow |c\rangle$  at frequencies  $\omega_P + \omega_L + R$ , left couple of thick arrows (orange on line) and  $\omega_P + \omega_L - R$ , right couple of thick arrows (red on line). Two couples of thin arrows (blue and violet on line), show the probe transition frequencies  $\omega_P - R$  and  $\omega_P + R$ , where gain is also possible.  $R = \sqrt{\Omega_P^2 + \Omega_L^2}$  is the generalized Rabi frequency.

from the exact analytic solution of the steady state master equation. Approximate formulas for the coherences are given by

$$\rho_{ab} = -\frac{2\Omega_P e^{i\varphi_P} [2(\Delta_L + \Delta_P) + i\gamma_{cb}]}{(\gamma_{ba} - 2i\Delta_P)[\gamma_{cb} - 2i(\Delta_L + \Delta_P)] + 4\Omega_L^2} \quad (5)$$

$$\rho_{ac} = -\frac{4\Omega_P \Omega_L e^{i(\varphi_P + \varphi_L)}}{(\gamma_{ba} - 2i\Delta_P)[\gamma_{cb} - 2i(\Delta_L + \Delta_P)] + 4\Omega_L^2} \quad (6)$$

Here  $\gamma_{cb}$  and  $\gamma_{ba}$  are spontaneous decay rates on the drive and the probe transitions, respectively,  $\Delta_P = \omega_{ab} - \omega_P$  and  $\Delta_L = \omega_{bc} - \omega_L$  are one-photon detunings between the laser frequencies  $\omega_P$  and  $\omega_L$  and the corresponding atomic frequencies  $\omega_{ab}$  and  $\omega_{bc}$ . The two-photon detuning  $\Delta_P + \Delta_L = \omega_{ac} - (\omega_P + \omega_L)$  contains the frequency  $\omega_{ac}$  of originally dipole-forbidden atomic transition  $|a\rangle \rightarrow |c\rangle$  indicating possible oscillations at that frequency. It is important to note that due to the presence of the exponent factor  $\exp[i(\varphi_P + \varphi_L)]$  in the numerator of Eq. (6), the coherence  $\rho_{ac}$  is *phase sensitive*. Varying the relative phase  $\Delta\varphi = \varphi_P + \varphi_L$  between the probe and the drive fields allows for an interchange between absorptive and dispersive line shapes of  $|a\rangle \rightarrow |c\rangle$  transition, defined by imaginary and real parts of the coherence  $\rho_{ac}$ , respectively. It is instructive to consider two particular cases of "bare" and "dressed"

two-photon resonances, when  $\Delta_P + \Delta_L = 0$  and  $\Delta_L + \Delta_P = \pm\Omega_L$ , respectively. At "bare" two-photon resonance  $\Delta_P + \Delta_L = 0$ , the coherence  $\rho_{ab}$  on the probe transition is small of the order of  $\Omega_P/\Omega_L^2$ . the coherence  $\rho_{ac}$  on the ACSA transition is proportional to  $e^{i\Delta\varphi}\Omega_P/\Omega_L$ , so that both absorption and dispersion can take small values between  $-\Omega_P/\Omega_L$  and  $\Omega_P/\Omega_L$ , depending on the relative phase  $\Delta\varphi$ . This accentuates the importance of the phase relation between the two laser fields and the phase sensitivity of the ACSA transition.

A different picture is obtained when the probe field is tuned in resonance with transitions between dressed states, i.e. when the two photon detuning equals the Rabi frequency of the driving field ("dressed" two-photon resonance). The dressed resonance condition and the coherences are given by

$$\Delta_L + \Delta_P = \pm\Omega_L \quad (7)$$

$$\rho_{ab} = \pm \frac{2e^{i\varphi_P}(\gamma_{cb} \mp 2i\Omega_L)\Omega_P}{2(\gamma_{ba} + \gamma_{cb})\Omega_L \pm i\gamma_{ba}\gamma_{cb}} \quad (8)$$

$$\rho_{ac} = \mp \frac{ie^{i(\varphi_P + \varphi_L)}\Omega_L\Omega_P}{2(\gamma_{ba} + \gamma_{cb})\Omega_L \pm i\gamma_{ba}\gamma_{cb}} \quad (9)$$

In this case both  $\rho_{ac}$  and  $\rho_{ab}$  are not small since they are proportional to the probe Rabi frequency  $\Omega_P$  rather than to the ratio  $\Omega_P/\Omega_L$  between the probe and the driving field Rabi frequencies, as in the above mentioned bare resonance case. This is confirmed by the exact analytical calculations as discussed below. Also gain and dispersion on the ACSA transition are not symmetric with respect to the bare two-photon resonance  $\Delta_P + \Delta_L = 0$ , as evident from Eq. (9).

To get a quantitative picture, the results of the exact analytical solution of the steady state master equation are shown in the following. Steady state coherence  $\rho_{ac}$  on the ACSA transition as a function of the probe detuning is shown in Fig. 4 at various values of the relative phase  $\Delta\varphi$ .

The coherence  $\rho_{ab}$  is drawn in 3D Fig. 5 as a function of the probe detuning  $\Delta_P$  and of the relative field phase  $\Delta\varphi$ . When the probe and the driving fields are *in-phase* ( $\Delta\varphi = 0$ ), there is a strong gain with negative dispersion slope at  $\Delta_P + \Delta_L = -\Omega_L$ , and absorption with normal dispersion at  $\Delta_P + \Delta_L = \Omega_L$ . Inverse picture is obtained when the probe and driving fields are *out of phase*, i.e.  $\Delta\varphi = \pi$ . If the field phases are  $\pm\pi/2$ -shifted, the absorption profile takes a dispersive shape while the dispersion behaves in absorptive-like manner

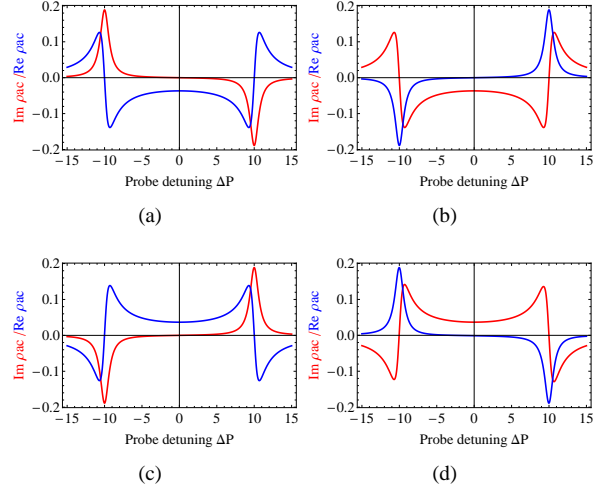


Figure 4: Gain (red line) and dispersion (blue line) at ACSA transition as a function of the probe detuning. Parameters:  $\gamma_{ba} = \gamma_{cb}$ ,  $\Omega_L = 10\gamma_{cb}$ ,  $\Omega_P = 0.37\gamma_{cb}$ ,  $\Delta\varphi = 0$  (a),  $\pi/2$  (b),  $\pi$  (c),  $3\pi/2$  (d).

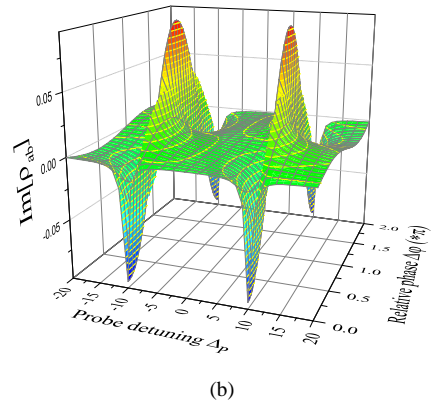
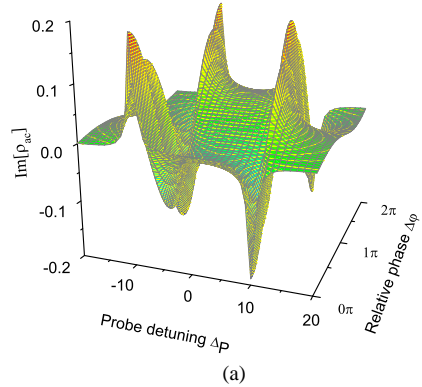


Figure 5: 3D plot of gain/absorption at ACSA (a) and probe (b) transition as a function of the probe detuning and of the relative field phase  $\Delta\varphi$ . Parameters:  $\gamma_{ba} = \gamma_{cb}$ ,  $\Omega_L = 10\gamma_{cb}$ ,  $\Omega_P = 0.37\gamma_{cb}$ .

- an indication of the quantum interference. Note the difference between the two transitions: the probe absorption  $Im[\rho_{ab}]$  is symmetric with respect to bare two-photon resonance  $\Delta_P + \Delta_L = 0$  so that there is either absorption or gain simultaneously on both side-bands  $\Delta_P + \Delta_L = \pm\Omega_L$ , while the coherence  $Im[\rho_{ac}]$  on the ACSA transition is antisymmetric with respect to the origin, so that there is always gain on one side-band and absorption on the other one. The frequency at which amplification takes place can be tuned by varying the driving field intensity because maximal gain is obtained at  $\Delta_P + \Delta_L = \pm\Omega_L$ .

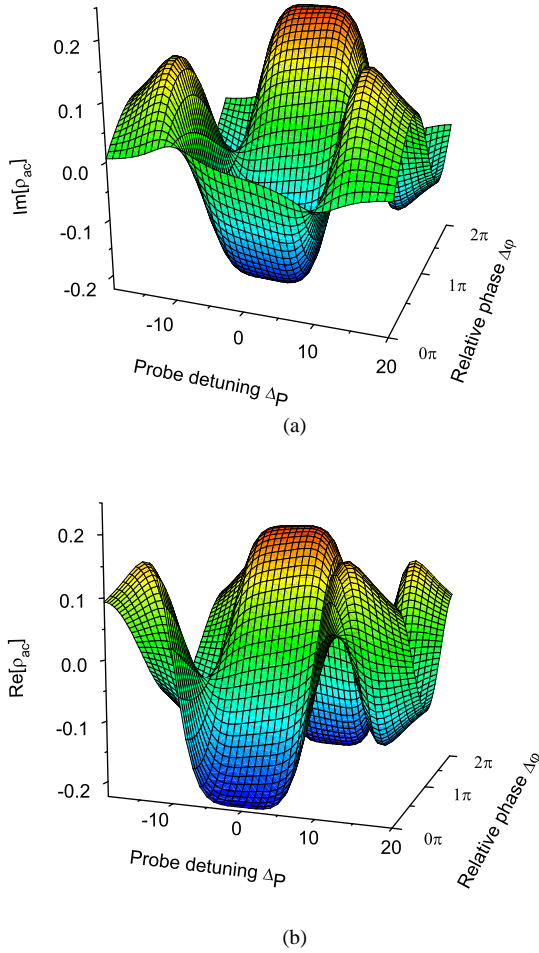


Figure 6: 3D plot of gain/absorption (a) and dispersion (b) at ACSA transition at strong probe field as a function of the probe detuning and of the relative field phase  $\Delta\phi$ . Parameters:  $\gamma_{ba} = \gamma_{cb}$ ,  $\Omega_L = 10\gamma_{cb}$ ,  $\Omega_P = 3.4\gamma_{cb}$ .

Another intriguing manifestation of quantum interference is obtained when the probe field is not weak

with respect to the driving one. Figure 6 shows flat-top behavior of both the absorption/gain and the dispersion at ACSA transition at strong enough probe field. Again the absorption/dispersion regime can be effectively controlled by the relative field phase  $\Delta\phi$ . Figure 7 demonstrates four essentially different cases controlled by the *phase shift* between the probe and driving fields: (i) reduced refraction index at  $\Delta\phi = 0$  (fields in-phase, Fig.7(a)), (ii) strong absorption with normal dispersion at  $\Delta\phi = \pi/2$  (Fig.7(b)), (iii) strongly enhanced refraction index at  $\Delta\phi = \pi$  (out-of-phase fields, Fig.7(c)), and (iv) strong gain without inversion and anomalous dispersion at  $\Delta\phi = -\pi/2$  (Fig.7(d)). The results shown in Figs. 7(c) and 7(d) are especially important as they hint for two interesting potential applications: laser or/and optical amplifier with a wide spectral range of operation (see Fig. 7(c)), and a controllable atomic dispersion in wide spectral range (see Fig. 7(d)).

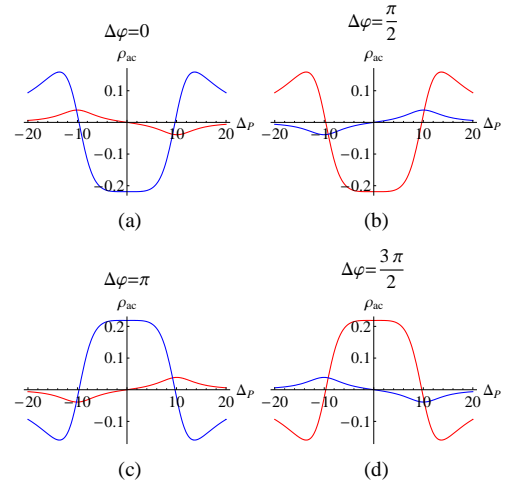


Figure 7: Flat-top behavior of gain/absorption (red line) and dispersion (blue line) on the ACSA transition at strong pump field at various values of relative field phase  $\Delta\phi$ . Gain (absorption) is obtained at positive (negative) values. (a) Suppressed refraction index at  $\Delta\phi = 0$ , (b) Strong absorption with normal dispersion at  $\Delta\phi = \pi/2$ , (c) Enhanced refraction index at  $\Delta\phi = \pi$ , (d) Gain without inversion with negative dispersion slope at  $\Delta\phi = -\pi/2$ . Note that the antisymmetric behavior of the gain is accompanied by symmetric behavior of the dispersion at specific phase values, and vice versa. Parameters:  $\gamma_{ba} = \gamma_{cb}$ ,  $\Omega_L = 10\gamma_{cb}$ ,  $\Omega_P = 3.4\gamma_{cb}$ .

#### 4. Absorption spectrum

To calculate the absorption spectrum, the master equation (2) with time dependent Hamiltonian (1) has been solved numerically and then Fourier transform has been taken. Figure 8 plots the spectrum of the coherence  $\rho_{ac}$  for various values of the probe detuning  $\Delta_P$ . As one

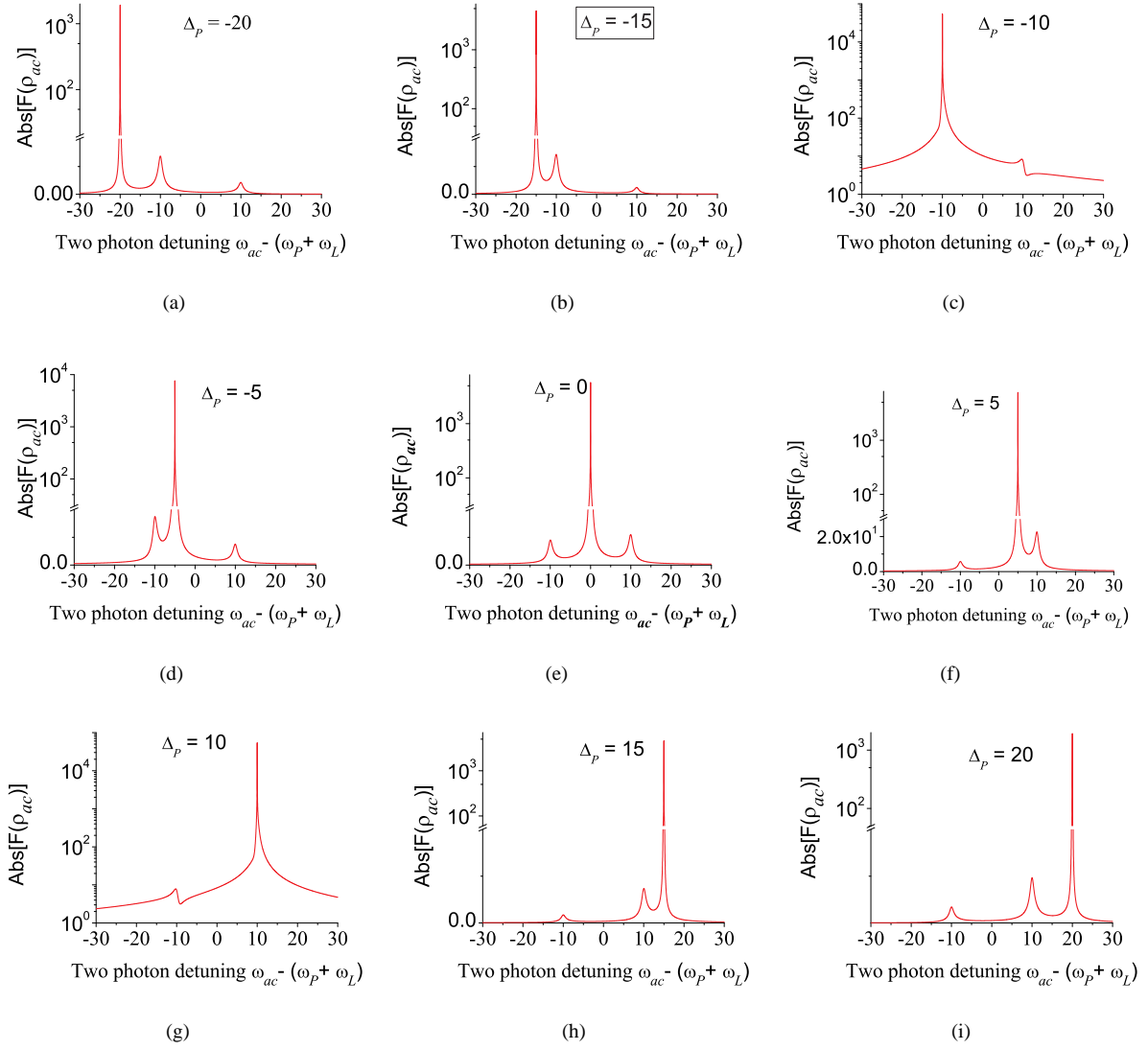


Figure 8: Absorption spectrum of  $|a\rangle \rightarrow |c\rangle$  ACSA transition. Note sharp strong peak at dressed two-photon resonance  $\Delta_p + \Delta_L = \pm\Omega_L$  (see parts c and g which are plotted in logarithmic scale). Parameters:  $\Omega_L = 10$ ,  $\Omega_p = 0.37$ ,  $\Delta\varphi = 0$ ,  $\Delta_L = 0$ ,  $\Delta_p = -20$  (a),  $-15$  (b),  $-10$  (c),  $-5$  (d),  $0$  (e),  $5$  (f),  $10$  (g),  $15$  (h),  $20$  (i).

can see, in addition to two resonances at Rabi-shifted transition frequencies  $\omega_{ac} \pm \Omega_L$ , a very sharp peak appears at  $\omega_{ac} + \Delta_P + \Delta_L$ . This peak becomes especially strong by a few orders of magnitude, at the "dressed" two-photon resonance, i.e. at  $\Delta_P + \Delta_L = \pm \Omega_L$  (see Figs. 8(c) and 8(g)). Interestingly, the peaks have extremely narrow line widths. We have found numerically that increasing accuracy of digital Fourier transform gives rise to vanishing line width, i.e. ideally, if one could perform Fourier transform with infinite accuracy, the peaks would look like  $\delta$ -function. This can be explained by the absence of mechanisms of line-broadening on the ACSA transition in this model. Indeed, there are neither dissipative processes which could contribute to line width, nor the field broadening as no field is applied to this transition. These will, of course, give a finite line width.

Sharp strong resonance in the spectrum of  $|a\rangle \rightarrow |c\rangle$  transition means that an efficient lasing is possible on this transition with extremely narrow spectral line. Moreover, such a laser would be tunable since its frequency can be controlled by varying both the frequency of either the driving or the probe laser, and by the intensity of the driving laser. Features of dark states and EIT are also obtained.

## 5. Conclusions

The ladder configuration of a three level system interacting with two laser fields has been studied. We have shown that strong coherence is established on the  $|a\rangle \rightarrow |c\rangle$  transition that originally was electric-dipole forbidden due to selection rules. However, the presence of two laser fields brakes the spherical symmetry and makes this transition dynamically allowed. Calculation of the coherences shows that ACSA (AC Stark Allowed) transition can exhibit such quantum interference related phenomena as gain without inversion, EIT, enhanced refraction etc. It is demonstrated that absorption/dispersion properties of ACSA transition are phase sensitive as they depend upon the relative phase of the probe and the drive laser fields and are changed at will. Subnatural linewidth resonances are found on ACSA transition enabling high resolution spectroscopy. This may also involve practical applications in Autler-Townes spectroscopy in atomic [21] and molecular [22] systems.

Strong gain without inversion found in a wide spectral range at strong probe laser field, is of particular interest as it opens a new perspective for creating ultra-short wavelength and X-ray lasers without inversion.

An important finding interesting for potential applications is simultaneous strong gain and negative dispersion slope, which means that an incident light may both be amplified and slowed down. This leads to significant changes in the group velocity in this range, in the speed of light etc. An occurrence of flat top dispersion accentuates these effects in wide range of detuning of the probe and the drive fields. These are important in broadband communications, Sagnac effects and other applications.

It should be noted that our results are applicable to the systems where all three transitions are electric dipole allowed, such as Ruby and other solid materials, and semiconductor quantum structures.

We propose to use femtosecond comb for the pump and probe lasers where phase relation among components can be determined. In such experiment one looks for radiation at the forbidden transition frequency.

## References

- [1] Elena Kuznetsova, Yuri Rostovtsev, Nikolai G. Kalugin, Roman Kolesov, Olga Kocharovskaya, and Marlan O. Scully. Generation of coherent terahertz pulses in ruby at room temperature. *Phys. Rev. A*, 74:023819, Aug 2006.
- [2] Yu-xi Liu, J. Q. You, L. F. Wei, C. P. Sun, and Franco Nori. Optical selection rules and phase-dependent adiabatic state control in a superconducting quantum circuit. *Phys. Rev. Lett.*, 95:087001, Aug 2005.
- [3] J. F. Dynes and E. Paspalakis. Phase control of electron population, absorption, and dispersion properties of a semiconductor quantum well. *Phys. Rev. B*, 73:233305, Jun 2006.
- [4] H. Shpaisman, A. D. Wilson-Gordon, and H. Friedmann. Electromagnetically induced waveguiding in double- $\lambda$  systems. *Phys. Rev. A*, 71:043812, Apr 2005.
- [5] U. Akram, J. Evers, and C.H. Keitel. Multiphoton quantum interference on a dipole-forbidden transition. *Journal of Physics B: Atomic, Molecular and Optical Physics*, 38(4):L69, 2005.
- [6] M. D. Frogley, J. F. Dynes, M. Beck, J. Faist, and C. C. Phillips. Gain without inversion in semiconductor nanostructures. *Nature materials*, 5:175–178, 2006.
- [7] J. F. Dynes, M. D. Frogley, J. Rodger, and C. C. Phillips. Optically mediated coherent population trapping in asymmetric semiconductor quantum wells. *Phys. Rev. B*, 72:085323, Aug 2005.
- [8] P. Kaer Nielsen, H. Thyrestrup, J. Mørk, and B. Tromborg. Numerical investigation of electromagnetically induced transparency in a quantum dot structure. *Opt. Express*, 15(10):6396–6408, May 2007.
- [9] E. Arimondo A.S. Sieradzan and M.D. Havey. Induced narrow resonances in two-photon excitation of atomic Cs. In *The 44-th Winter Colloquium on Physics of Quantum Electronics'14, Book of Abstracts*, Snowbird, Uta, 2014.
- [10] S. H. Autler and C. H. Townes. Stark effect in rapidly varying fields. *Phys. Rev.*, 100:703–722, Oct 1955.
- [11] M. O. Scully and M. S. Zubairy. *Quantum Optics*. Cambridge University Press, 1 edition, September 1997.

- [12] Michael Fleischhauer, Atac Imamoglu, and Jonathan P. Marangos. Electromagnetically induced transparency: Optics in coherent media. *Rev. Mod. Phys.*, 77:633–673, Jul 2005.
- [13] J Mompert and R Corbaln. Lasing without inversion. *Journal of Optics B: Quantum and Semiclassical Optics*, 2(3):R7, 2000.
- [14] A Andr, M D Eisaman, R L Walsworth, A S Zibrov, and M D Lukin. Quantum control of light using electromagnetically induced transparency. *Journal of Physics B: Atomic, Molecular and Optical Physics*, 38(9):S589, 2005.
- [15] A. S. Zibrov, M. D. Lukin, L. Hollberg, D. E. Nikonov, M. O. Scully, H. G. Robinson, and V. L. Velichansky. Experimental demonstration of enhanced index of refraction via quantum coherence in Rb. *Phys. Rev. Lett.*, 76:3935–3938, May 1996.
- [16] J. Vanier, M. Levine, D. Janssen, and M. Delaney. The coherent population trapping passive frequency standard. In *Precision Electromagnetic Measurements, 2002. Conference Digest 2002 Conference on*, pages 580–581, June 2002.
- [17] Aldo Godone, Salvatore Micalizio, Filippo Levi, and Claudio Calosso. Physics characterization and frequency stability of the pulsed rubidium maser. *Phys. Rev. A*, 74:043401, Oct 2006.
- [18] Clude Cohen-Tanudji, Jacques Dupont-Roc and Gilbert Grynberg. *Atom-Photon interactions: Basic Processes and Applications*. John Wiley, Chapter VI, 1992.
- [19] D. Braunstein and R. Shuker. Absorption with inversion and amplification without inversion in a coherently prepared  $\nu$  system: A dressed state approach. *Physical review A*, 64:053812–1 – 053812–12, 2001.
- [20] D. Braunstein and R. Shuker. X-ray laser without inversion in a three-level ladder system. *Phys. Rev. A*, 68:013812, Jul 2003.
- [21] B. K. Teo, D. Feldbaum, T. Cubel, J. R. Guest, P. R. Berman, and G. Raithel. Autler-townes spectroscopy of the  $5S_{1/2} - 5P_{3/2} - 44D$  cascade of cold  $^{85}\text{Rb}$  atoms. *Phys. Rev. A*, 68:053407, Nov 2003.
- [22] Ruth Garcia-Fernandez, Aigars Ekers, Janis Klavins, Leonid P. Yatsenko, Nikolai N. Bezuglov, Bruce W. Shore, and Klaas Bergmann. Autler-townes effect in a sodium molecular-ladder scheme. *Phys. Rev. A*, 71:023401, Feb 2005.